

Electronic structure of 5d transition metals adsorbed on the stoichiometric (110) rutile surface

L. Thiên-Nga* and A. T. Paxton

Atomistic Simulation Group, Department of Pure and Applied Physics, Queen's University, Belfast BT7 1NN, United Kingdom

(Received 22 September 1997; revised manuscript received 26 May 1998)

Electronic structures and charge transfers of 5d transition-metal rows (Ta to Au), adsorbed on the stoichiometric (110) surface of TiO₂, have been calculated *ab initio* in a model configuration. Their detailed analysis clarifies the concepts of oxidation and reduction of the rutile for adsorption on the fivefold titanium site. It is found that no large charge transfers occur, and that there is covalent bonding between the metal and the titanium neighbor. The variations of the charge transfers, although small, correlate with noticeable variations of the core-level shifts and of the adsorption energies. [S0163-1829(98)11039-1]

INTRODUCTION

Adsorption of metals on rutile involves a variety of phenomena at different scales; yet, despite the complexity, one is tempted to extract general trends across the Periodic Table. For example, while the noble metals tend to cluster on the rutile substrate,^{1,2} wetting is said to be favored the higher the reactivity of the metal towards oxygen.² Deposition of a reactive metal, from the point of view of the electronic structure, would also be accompanied by the appearance of new titanium oxidation states. One would therefore like to see, in a simpler situation, to what extent such concepts as correlation of the observed behavior with metal-oxygen affinity and titanium reduction apply at the atomic level, in terms of electronic structure.

Technologically, metals on TiO₂ have raised much interest and are being used as photocatalysts, chemical sensors, and heterogeneous catalysts under reducing atmospheres. In all these applications, a major point is the interplay of the adsorbed substance with the electronic structure of the stoichiometric or defective TiO₂ system. Experimentally, surface-science spectroscopies now allow investigation of ultrathin grown metal overlayers. A systematic body of experimental data has been formed over the years,¹⁻³ and state-of-the-art techniques are currently being used in this area.^{4,5} There is also the hope that local probes such as scanning tunneling microscopy (STM) will yield information, at the atomic scale, on the electronic structure of such systems.^{6,7} The need for a proper description of interactions at an atomic scale has recently even motivated studies of catalysis on noble metal/TiO₂ materials with a metal coverage in the submonolayer range.⁸

On the modeling side, metal/oxide studies have concentrated on Al₂O₃ and MgO, where the cation is in a fixed oxidation state.^{9,10} The theoretical interest in metal on rutile systems arises from the different oxidation states of titanium in titanium oxides.¹¹ In a purely qualitative approach, one would think that quantities such as the ionization potential of the metal (its resistance to giving up an electron), or, conversely, its oxygen affinity, can be related directly to metal-substrate charge transfer. In practice, though, the charge transfer, relative positions of the densities of states, and, more generally, the energy and spatial distribution of the charge can only be known through a self-consistent calculation

of the charge and the potential simultaneously.⁹ This can be done through self-consistent semiempirical models¹² or *ab initio* calculations;^{13,14} in the present study an *ab initio* approach is used.

We would like to emphasize also that, so far, few comparisons between different metals on a single oxide were made, because bulk interfaces were considered and, therefore, the metal had to be chosen so that lattice matching was favorable. Our calculations relate to the early stages of metal deposition: there is at most one metal atom per elementary surface unit. In such configurations it is possible to perform calculations for a series of metals.

Using the FP-LMTO method,¹⁵ we have investigated bonding at a special site of the TiO₂(110) surface for seven 5d transition metals—Ta, W, Re, Os, Ir, Pt, and Au—in order to compare results across the series for the same geometry. In Sec. I, preliminary bulk and clean surface calculations are summarized; the geometry of the cells and computational details are given. In Sec. II, the effects of metal adsorption on the substrate density of states are shown, as well as two examples of the detailed interactions of the metal with surface atoms. In Sec. III, charge transfers and bonding across the series are analyzed. We describe how the relative positions of the atomic core levels reflect the electrostatics of the system and are helpful to explain the variations of the density of states for some atoms. Section IV completes the picture with calculations for half-coverage systems and spin-polarized calculations. Finally, the results are discussed in Sec. V.

I. BACKGROUND FOR THE CALCULATIONS

The reader is referred to Ref. 11 for details on the bulk and (110) stoichiometric surface, as well as the reduced 1 × 1 surface. Still it might be useful to summarize the main features of the electronic structure in relationship with the surface geometry. The rutile structure can be seen as built from octahedra (Fig. 1), where each titanium has four equatorial and two apical oxygens as nearest neighbors. The energy bands of most interest are, essentially, a low-lying narrow O 2s band and a filled valence band with mainly O 2p character. A gap of 1.7 eV separates this valence band from the mainly Ti d empty conduction band. Nevertheless, hybridization between Ti d and O 2p orbitals cannot be ne-

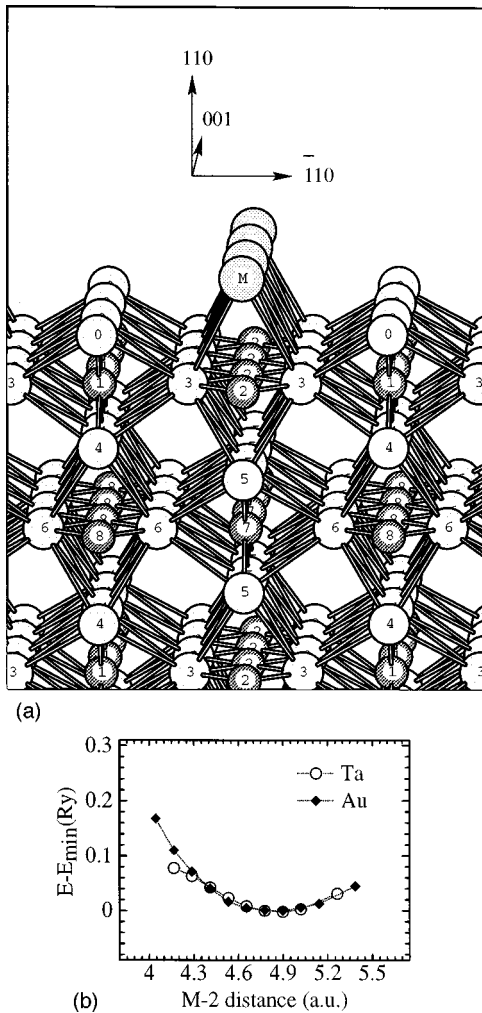


FIG. 1. (a) Supercell geometry for the full row of metal atoms (medium gray) adsorbed on the stoichiometric (110) surface: titanium atoms (dark gray) are at the center of oxygen (light gray) octahedra. (b) M to Ti(2) distance minimization, using four k points, for metals at the extremities of the series.

glected. There is a substantial amount of covalency in TiO_2 ; even though there is a degree of arbitrariness when attributing charge to one atom or the other through projection on the atomic basis, it is found that Ti bears a 1.2^+ charge and O is 0.6^- , instead of the formal ionic charges 4^+ and 2^- .

There is agreement on the fact that the (110) stoichiometric surface is the most stable surface for the compound. Figure 1 shows that there are two inequivalent titanium atoms on the surface: one of them is at the center of an octahedron which the (110) plane “cuts,” and is fivefold coordinated; the other one is sixfold coordinated, bound to two oxygens which stand above the surface and are named “bridging oxygens.” The density of states for the surface retains the features of the bulk density: there are no surface states in the gap. Changes in the density of states compared to the bulk are bound to arise from coordination changes and modifications of the Madelung potential at surface sites. They can be analyzed by examining the local densities of states (LDOS) (see Fig. 2). We have checked that the electrostatic shifts decay rapidly with distance from the surface: for a five-layer slab, they are less than 0.2 eV at the center of the slab.

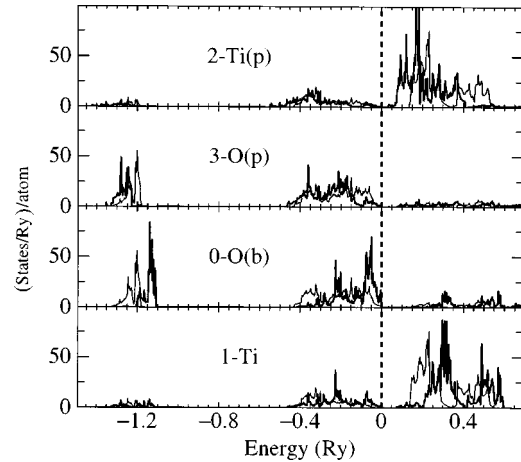


FIG. 2. Projected Mulliken densities of states of surface sites of the clean rutile surface (thick line): fivefold-titanium (2), plane oxygen (3), bridging oxygen (0), and sixfold-titanium (1). From left to right, the peaks have O $2s$, O $2p$, and Ti $3d$ character. The dashed line is the upper boundary of the filled levels. The corresponding bulk densities of states are shown (thin line), which shows the significant Madelung shifts occurring at the surface.

We chose to investigate a site where the metal sits on top of the titanium. The supercell is a three-layer slab with a metal atom on top of the fivefold titanium (Fig. 1), which completes the surface octahedron. The geometry is, on one hand, simple and computationally reasonable, and on the other hand, it has been shown experimentally that Pt atoms tend to sit on that site at very low coverage.¹⁶ One should emphasize that this study does not aim at finding the minimum energy configuration of the seven metal-oxide systems. This cannot be done for a full series of elements. There is a deep reason for using only one geometrical configuration. In the real world, the adsorption geometries are likely to be (at least some of them) very different and hardly comparable, so that it would be impossible to really separate the effects of metal-oxygen affinity and adsorption geometry. This study is a model calculation where we would rather see trends in the details of the interactions for the same geometry in order to compare “like with like,” at a site which is plausible for some of the elements.

With the periodic boundary conditions, we are actually dealing with a row of metal atoms with a spacing equal to the lattice parameter c (5.5 a.u., while the average nearest-neighbor distance of these metals is 5.3 a.u.). Given the conflicting results on the surface relaxations in the community at the beginning of our study, we chose to set the rutile in an unrelaxed configuration. Some calculations were then carried out to test the influence of surface relaxations. For the metal atom, the distance to the substrate is kept constant across the series at 4.85 a.u. above the plane, the distance being determined by minimization for Au with only four k points used in the Brillouin-zone integration. Again this was a compromise to achieve a rough local minimization with an affordable amount of computation. It can be seen indeed in Fig. 1(b) that this distance is not unreasonable for Ta either, at the other end of the series.

The calculations use the FP-LMTO method, which is an all-electron *ab initio* density-functional theory approach within the local (spin) density approximation [L(S)DA]. In

this method the core is allowed to relax, but is treated as spherically symmetric. All relativistic effects except spin-orbit coupling are included. For LSDA calculations we use the functional of von Barth and Hedin, modified by Moruzzi, Janak, and Williams.¹⁷ For the technical details regarding the choice of orbitals, for example, the reader is referred to Ref. 11, as the same basis set was chosen for this study. For the metal, 6*s*, 6*p*, and 5*d* levels were taken as valence levels and 5*s*, 5*p* levels were included in the semicore. It was found that, in the plane of the surface, 14 × 14 *k* points on the main panel were needed to achieve a convergence of 1 mRy. A set of calculations where every other metal atom was removed was also made, with spin polarization included. The dimensions of the supercell are doubled along the *c* axis, while other dimensions are unchanged. The metal free atom reference energy was determined from atomic calculation. Once the calculation is performed, the local density of states (LDOS) and crystal orbital overlap population (COOP) for each $\alpha = lm$ or *l* index are obtained through a Mulliken analysis. If an eigenstate ψ_n is written in the basis set as

$$\psi_n = \sum_{i,\alpha} a_{i,\alpha}^n |i,\alpha\rangle,$$

where *i* is the site index, then

$$n_i(E) = \sum_n \sum_{\alpha} |a_{i,\alpha}^n|^2 \delta(E - E_n) + \sum_{\alpha} \sum_{j,\beta} \sum_n \bar{a}_{i,\alpha}^n S_{i\alpha,j\beta} a_{j,\beta}^n \delta(E - E_n)$$

defines the Mulliken density of states projected onto the basis function $|i,\alpha\rangle$ and

$$n_{i\alpha,j\beta}(E) = \sum_n \bar{a}_{i,\alpha}^n S_{i\alpha,j\beta} a_{j,\beta}^n \delta(E - E_n),$$

where $S_{i\alpha,j\beta}$ is the overlap integral between $|i,\alpha\rangle$ and $|j,\beta\rangle$ defines the COOP between sites *i* and *j*.

Finally, electronic core levels are given as output of these calculations; their relative positions can then be compared between different calculations.

II. EFFECTS OF METAL ADSORPTION ON THE DENSITY OF STATES

When metal atoms are deposited in the trough between the bridging oxygen rows, on top of every fivefold titanium, the metal-metal distance along [001] allows dispersion in this direction. In the case of tantalum, after iteration to self-consistency, the metal conduction band sits in the middle of the rutile band gap. The adsorbed metal induces new states on the substrate, situated in the gap [Fig. 3(a)]. These states, which were discovered by Heine¹⁸ in the context of metal-semiconductor interfaces, are called MIGS (metal-induced gap states). These mainly appear on the surface fivefold titanium. A more detailed picture of the interaction is given by the overlap spectral density (COOP's) (Fig. 4). The interaction happens near the Fermi level, in the energy window where MIGS have appeared. It involves mainly tantalum and

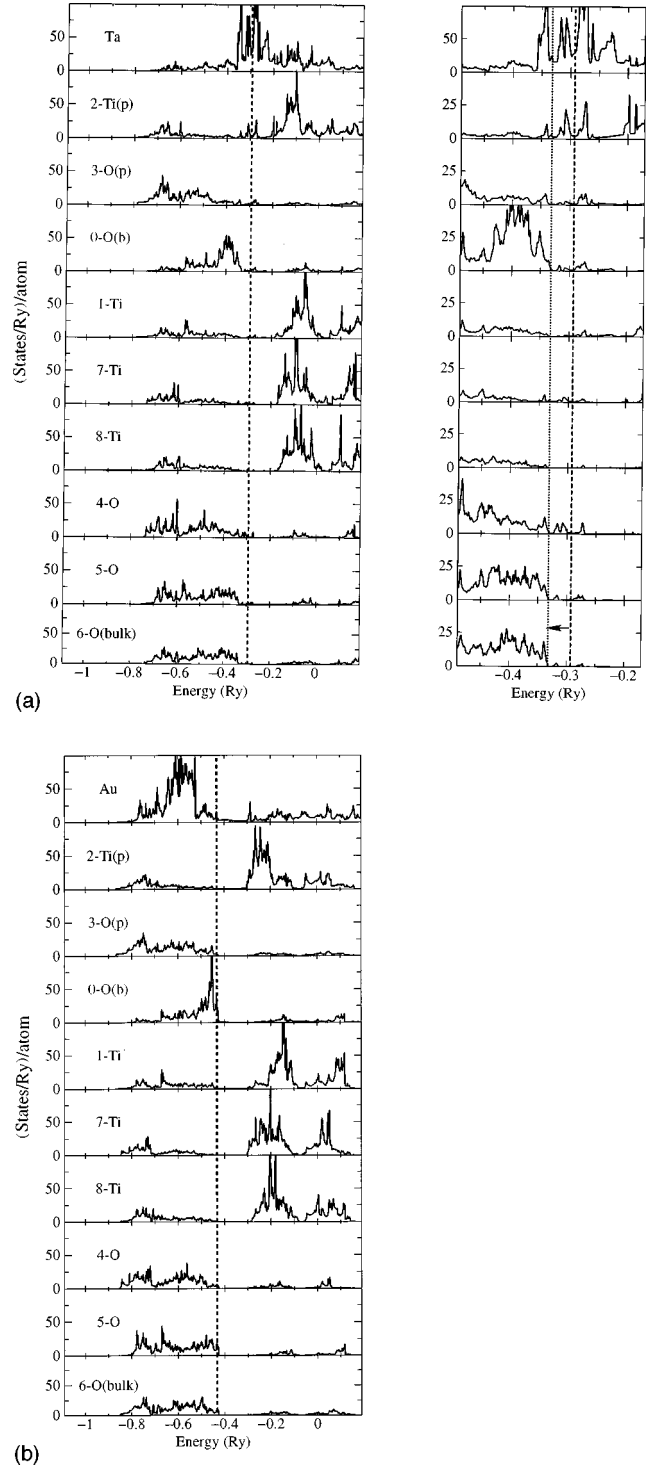


FIG. 3. Tantalum row: projected Mulliken densities of states. (a) Left panel, projected Mulliken densities of states. The dashed line represents the Fermi level, drawn between the mainly oxygen 2*p* valence band and the mainly Ti 3*d* conduction band. The origin of the energies is arbitrary. Note the covalency of the compound. The tantalum density of states sits in the middle of the gap. Right panel, enlargement showing the metal-induced gap states (MIGS) from the top of the center oxygen valence band (dotted line) to the Fermi level (dashed line). (b) Gold row, projected Mulliken densities of states. In this case the metal density of states is aligned with the valence band.

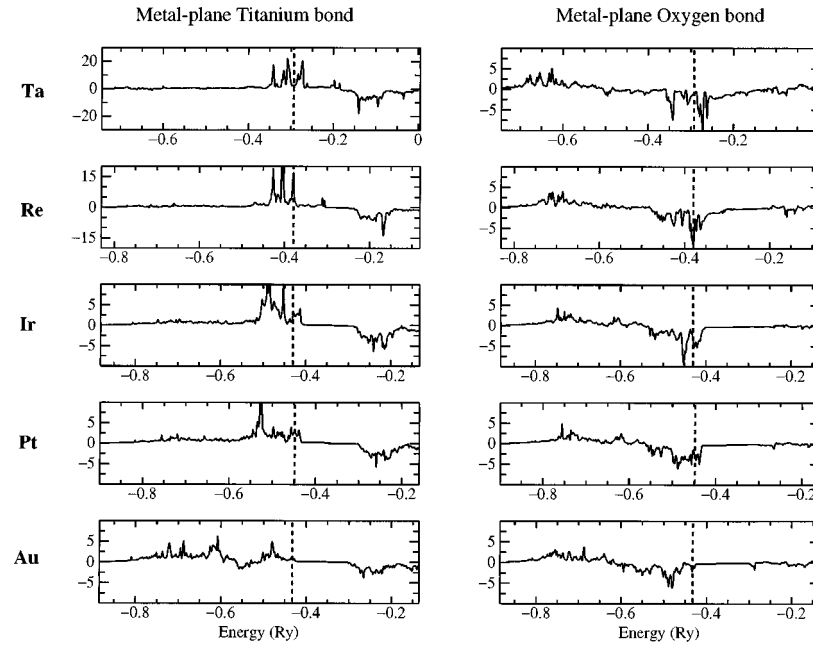


FIG. 4. Trends of the COOPS across the series. Left panel, metal-Ti(2) COOPS (in a.u.), showing the progressive filling of bonding levels and increase in the splitting of the bonding-antibonding groups. Right panel, metal-O(3) COOPS, showing the progressive filling of the antibonding levels.

titanium d orbitals, which can also be visualized by plotting the charge density associated with these states: in Fig. 5(a) the predominantly $d_{3z^2-r^2}$ character of the metal orbitals is shown. Clearly there is covalent bonding, and COOP's show the two groups of bonding and antibonding levels formed by the tantalum and titanium d levels. In this tantalum case, the bonding levels are partially filled.

For gold, at the other end of the series, the situation is different: metal d levels sit much lower relative to the substrate, and, as a consequence, no MIGS are formed [Fig. 3(b)]. Looking at the COOP's, the metal and titanium interact on a broader energy window, centered on the valence band. Around the bonding peak, an energy window with a

width comparable to the tantalum case was chosen to plot the charge-density map [Fig. 5(b)]. Now the metal d orbitals involved have a different symmetry. Compared to tantalum, the average level of the antibonding orbitals is shifted downwards (≈ 50 mRy), when the Fermi levels are aligned. More significantly, the spacing between bonding and antibonding groups has increased by, roughly, 200 mRy. This is consistent with a covalent picture of the metal-titanium bond, using lower d levels for gold than for tantalum [Fig. 6(a)]: as an indication, the difference in the first ionization potentials of gold and tantalum is about 100 mRy. For all metals, interaction with oxygen is essentially interaction with the in-plane oxygens. It is bonding at the bottom of the valence band, and

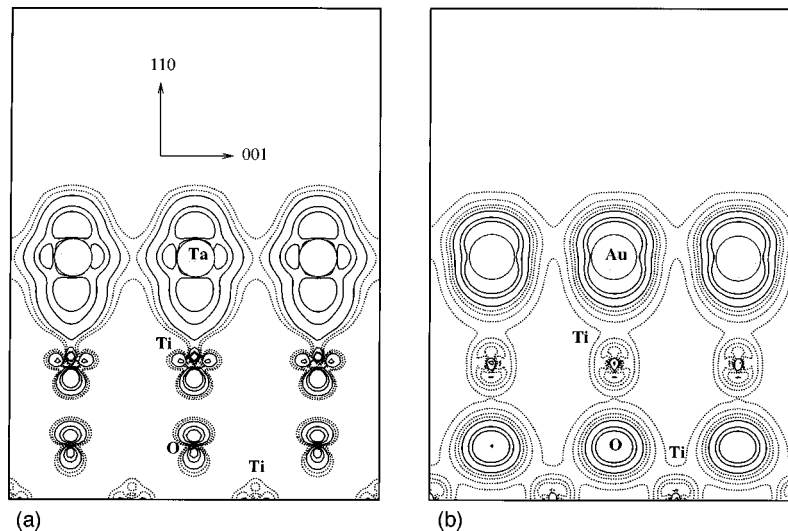


FIG. 5. Cross section of the energy-resolved charge densities along the metal row. (a) Charge integrated within the tantalum MIGS window. Density contours: $(5-7) \times 10^{-3} e^- / (\text{a.u.})^3$, dotted line; $(1-3) \times 10^{-2} e^- / (\text{a.u.})^3$, solid line. (b) Charge integrated around the "bonding peak:" (-0.62 to -0.60 Ry). Density contours: $(2-7) \times 10^{-3} e^- / (\text{a.u.})^3$, dotted line; $(1-3) \times 10^{-2} e^- / (\text{a.u.})^3$, solid line. Note the covalency between Ti and O.

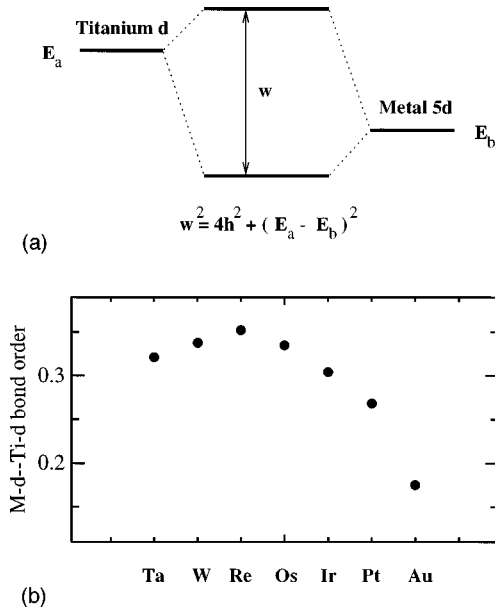


FIG. 6. (a) Spacing between bonding and antibonding energy levels in a molecular orbital picture. h = hopping integral. (b) Metal d -titanium d bond order (a.u.) across the series in the full-row configuration. Note the parabolic behavior.

antibonding close to the Fermi level; the mean spacing between bonding and antibonding groups diminishes by 50 mRy from the beginning to the end of the series, while antibonding levels get progressively filled.

III. CHARGE TRANSFERS AND CORE-LEVEL SHIFTS

By integrating the projected density of states $n_i(E)$, the distribution of the charge by atom is obtained. Although there is a degree of arbitrariness as in the choice of the LMTO basis, the projection basis itself does not change from one calculation to another so that we can then compare the series of results. To get the atomic charges, O $2s$ as well as O $2p$ levels were included. By subtracting the atomic charges obtained for the clean surface from the atomic charges with adsorbed metal, a charge transfer is calculated, as well as its splitting among the different surface atoms.

Figure 7 shows the variations of the transfer for the series of elements. The total transfer to the substrate, in absolute value, is always small, less than $0.2e^-$; it becomes negative (oxidizing) towards the noble metals.

At the center of the slab, the charge transfer is negligible ($<0.02e^-$), as well as for the in-plane oxygen (3). The main transfers occur for the bridging oxygen (0) and the corresponding subsurface oxygen (4), for the fivefold titanium (2) and the sixfold titanium below the bridging oxygen (1). The fivefold titanium gains electrons while the other titanium loses some. It is striking that all transfers are almost constant, except for the bridging oxygen and the fivefold titanium, the charge of which decreases with the number of transition-metal valence electrons. The general trend of the transfer is due to the variation of the bridging oxygen and titanium charge. The increase by +0.5 eV of the core-level shift for the bridging oxygen, going from Ta to Au, is consistent with the decrease of the charge transfer on this atom,

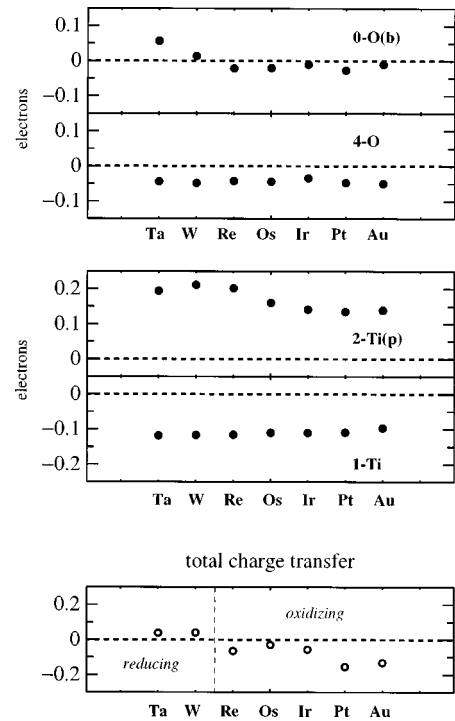


FIG. 7. Full-row charge transfers, showing the transition from reducing to oxidizing behavior. Positive sign: electrons *gained* by the substrate on adsorption. The variation of the total transfer can be attributed to the fivefold titanium and the bridging oxygen.

although this charge transfer is quite small in any case; this is also true of the fivefold titanium core-level shifts.

Integrating the COOP's, the variations of the bond orders for the metal-titanium and metal-oxygen interactions can be followed. For titanium [Fig. 6(b)], the bond order is dominated by metal- d /titanium- d interaction, which, like elemental transition metals, goes through a parabolic maximum in the middle of the 5d row. The metal-oxygen bond order is essentially metal-in-plane oxygens interaction (the length of these bonds is 5.2 a.u., the metal-bridging oxygen distance is 6.2 a.u.) and is roughly a quarter of the metal-titanium interaction. As noted before, going towards the noble metals, antibonding states are filled, so that the bond order decreases.

Upon metal adsorption, the electrostatic shifts described in Sec. I are liable to be modified by both screening and charge transfer. The shifts of oxygen $1s$ levels (relative to the oxygens in the middle of the slab, taken as the bulk reference) and the shifts of titanium $1s, 2s, 2p$ (relative to a selected titanium in the middle of the slab) have been determined (Fig. 8). They provide a more precise view of the electrostatics of our system, and, therefore, also of the alignment of the densities of states at the Fermi level.

Compared to the clean surface, the oscillations of the shifts with depth due to differences in the Madelung potentials are retained. Nevertheless, the amplitudes of these shifts are different, even when total charge transfer is close to zero, because of the screening due to the adsorbed atom, and because a redistribution of the charges occurs among the surface and subsurface atoms as analyzed previously. Despite the small charge transfers, shifts can vary by values up to 1 eV. Clearly the interaction with the metal shifts the fivefold

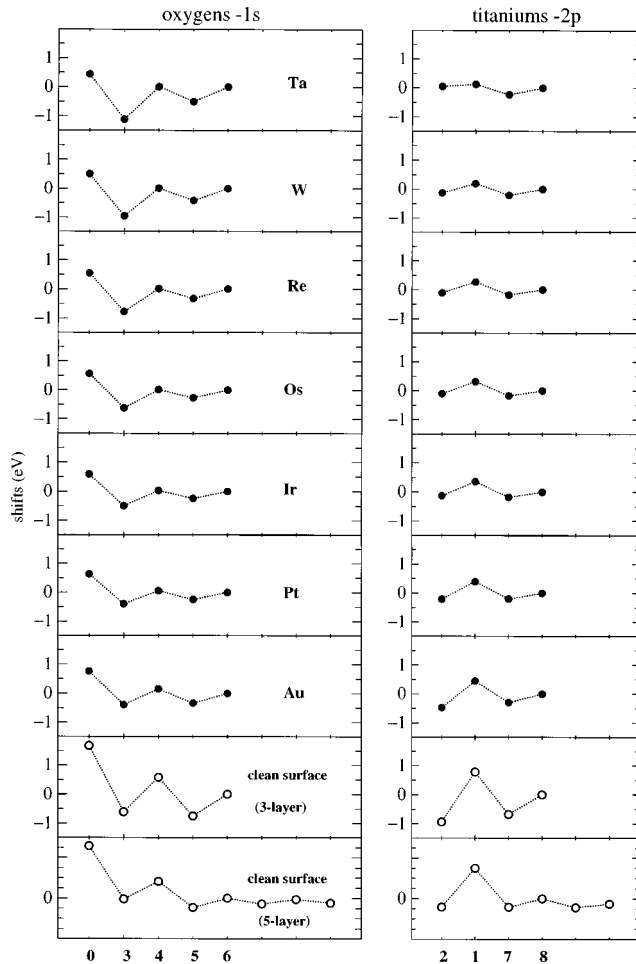


FIG. 8. Shifts of the oxygen $1s$ and Ti $2p$ core levels, as a function of the site, across the series. (0) bridging oxygen, (3) plane oxygen, (2) fivefold titanium, (1) sixfold titanium.

titanium (atom 2) energy levels upwards, particularly at the left of the series, while the contrary happens to the sixfold titanium (1). For oxygen atoms, the presence of adsorbed metal dampens the core-level shifts. This information shows the part played by the Madelung shifts on the local densities of states, when going from Ta to Au: the $2s$ level is shifted exactly by the value of the $1s$ shifts, and so is the valence-band peak (Fig. 9).

The changes correlate with the charge transfer to the bridging oxygen: for Au the charge is similar to the charge for the neutral surface, and the valence-band peak is close to the Fermi level, too. Once the electrostatic shifts are set, there is still a degree of freedom left with the charge transfer, or, equivalently, the position of the Fermi level. Indeed, taking the center oxygen $1s$ or $2s$ level as a reference, it can be seen (Fig. 9) that this position decreases smoothly by 30 mRy (0.4 eV) from Ta to Pt. The result of these variations of the electrostatic shifts, on one hand, and of the position of the Fermi level, on the other hand, is that, in the case of Ta, a separation distance of 40 mRy (0.6 eV) appears between the top of the substrate valence band and the Fermi level; or, using the language of semiconductors, the Fermi level is pinned in the middle of the gap, giving rise to some band bending. This band bending can be seen with W too, then disappears for the other metals.

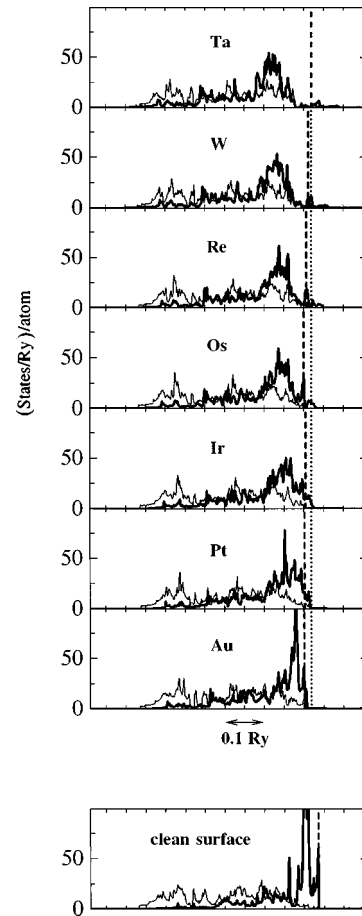


FIG. 9. Relative positions of the bridging oxygen (0) (thick line) and bulk oxygen (8) (thin line) valence bands and Fermi levels (dashed line). The oxygen $1s$ levels for bulk oxygen have been aligned. The dotted line is the position of the tantalum Fermi level. Note, across the series, the changes in the center of gravity of the band for (0), the disappearance of the offset from the Fermi level, and the lowering of the Fermi level.

IV. REDUCING THE COVERAGE: ADSORPTION ENERGIES, EFFECT OF SPIN POLARIZATION

Recently the issue of spin polarization in rutile systems was raised in a few papers.^{11,19–21} Particularly, it is remarkable that, in the K-TiO₂(001) Hartree-Fock study both spin polarization and charge transfer were found to be large.¹⁹

In our case of tantalum, the previous calculation (full-row geometry) was also performed within LSDA. Calculations were then performed for a half-coverage, with every other atom removed from the metal row along [001], so that dispersion along the metal row is strongly reduced. In that configuration, atoms in the second cell along [001], with no $5d$ -metal atom above, were labeled as in the first cell but with primes. For this low coverage “broken-row” configuration too, both non-spin-polarized and spin-polarized calculations were performed and compared. In both spin-polarized calculations the tantalum acquires a moment. Nevertheless, the substrate atoms are very weakly spin-polarized. We can compare the results with our previous study¹¹ of the (110) 1×1 reduced surface, which is a strongly reduced system; it was found there that the most reduced surface atom acquires $0.2e^-$ and a moment of $1.2\mu_B$ coming from spin polarization

TABLE I. Comparison between non-spin-polarized and spin-polarized tantalum “broken-row” calculations.

Atom	Charge transfer	Charge transfer	Moment
Ta	-0.047	-0.047	2.737
Ti(2)	0.316	0.210	0.271
Ti(1)	-0.092	-0.085	0.005
Ti(2')	0.069	0.043	0.033
O(0)	0.073	0.088	-0.084
O(5)	0.008	-0.048	0.065

of 3d titanium orbitals. It appears, therefore, that, in the case of the tantalum, where the total charge transfer is small and reduction is weak, the charge transfer to the fivefold titanium is nevertheless the same as in the reduced surface. Finally, if we compare broken-row and full-row configurations, the tantalum moment drops to $1.3\mu_B$ and the Ti(2) moment to $0.2\mu_B$, in accordance with the idea that magnetism should be lessened by dispersion along the metal row. The charge transfers are similar to within a tenth of an electron (see Table I). Also, as the total charge transfer is smaller, the band bending decreases from 0.6 eV to 0.3 eV for the lower coverage.

Broken-row spin-polarized calculations were then performed for the seven elements. Using LSDA calculations for the free atoms as a reference, adsorption energies were then calculated, and the charge transfers compared with results for the previous coverage.

For all metals the metal moment is found to be important: it is less, but follows the trend of the free atom moments. This induces small moments on the titanium below the metal, but the charge transfers are still very similar to the full-row non-spin-polarized calculations (Fig. 10 and Table II).

The adsorption energy (Fig. 11) varies from 5.9 to 9.5 eV/adsorbed atom. It is larger for the noble metals (Table III).

V. DISCUSSION

Deposition of a transition metal on TiO_2 is often viewed as a redox reaction: in the case of a very reactive metal (such as Hf), a fraction x of the oxygen forms a new oxide (HfO_2) with the metal, whereas the substrate is reduced to TiO_{2-x} . In many cases, though, there is no evidence of the formation of a new phase, but metal adsorption induces changes on the substrate. In these cases reduction of the substrate might occur by transfer of charge from the reactive metal to the titanium atoms; such a charge transfer could explain the appearance of a new titanium oxidation state suggested by spectroscopic experiments.^{2,3}

Although the temperature and geometry of the experiments cannot be represented in the modeling, we expect that analysis of ground-state calculations can give a clearer picture of the role of oxygen in the reduction/oxidation process in our simplified case, and for the site we have chosen; the charge transfers and the core-level shifts can be analyzed and compared in a detailed way.

For our chosen adsorption site, there is a covalent metal-oxygen interaction. As could be seen in Secs. II and III, this

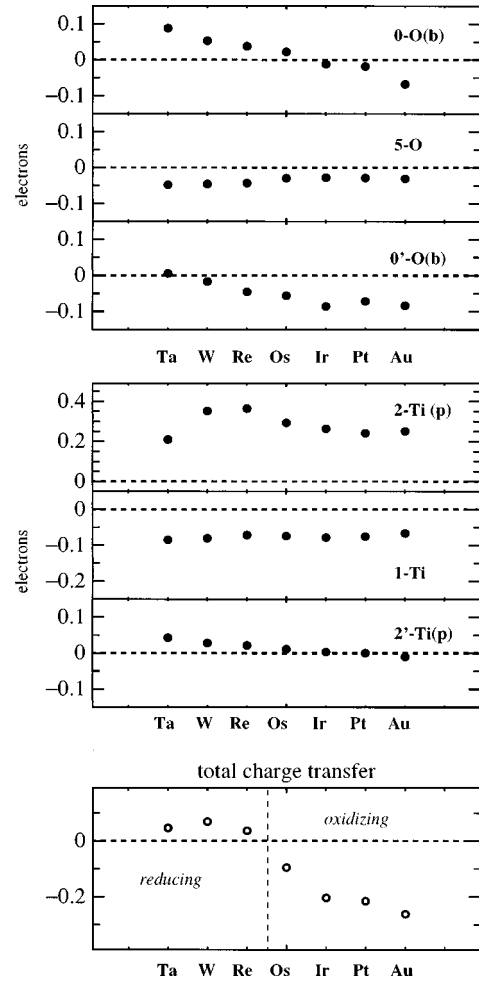


FIG. 10. Broken-row charge transfers. The variation of the total transfer can be attributed to the fivefold titanium and the bridging oxygens.

is mainly metal-in-plane oxygens interaction, and its bond order is at most a quarter of the metal-titanium one. The metal-oxygen bond order decreases through the series as antibonding levels get filled. This behavior, which is expected from a simple molecular orbital diatomic molecule diagram, was noted before in semiempirical calculations of 3d transition metals on Al_2O_3 .^{13,14} Nevertheless, the bond order and the adsorption energy do not follow the same trend; for this site bonding with the in-plane oxygens is not the dominant component in the adsorption energy. Apart from the formation of covalent bonds between the adsorbed metal and the in-plane oxygens, an additional effect of metal adsorption on

TABLE II. “Full-row” calculations. Charges are in electrons; only transfers superior to $0.04e^-$ are mentioned. Moments are in units of μ_B .

Atom	Charge transfer	Charge transfer	Moment
Ta	-0.049	0.027	1.319
Ti(2)	0.170	0.166	0.213
Ti(1)	-0.115	-0.119	0.009
O(0)	0.080	0.046	-0.030
O(5)	-0.076	-0.076	0.076

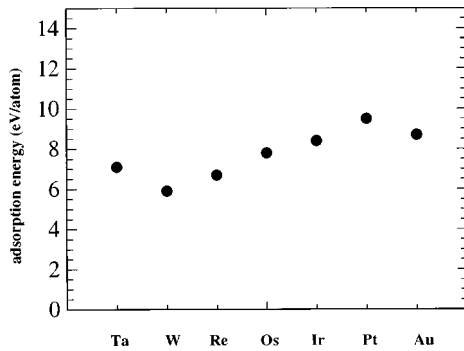


FIG. 11. Adsorption energies for the broken rows.

oxygen states is the variation of the bridging oxygen charge across the series: while covalent interaction involves nearest oxygen atoms, the electrostatic shifts give rise to varying charge transfer to the further oxygen, and this variation is in fact responsible for the decreasing trend of the total charge transfer.

On the question of charge transfer it might be helpful to recall a couple of results.⁹ For the calculations performed so far of metals on stoichiometric wide band-gap oxides (MgO or Al_2O_3), the charge transfer is always found to be small (≈ 0.01 to $0.1e^-$).^{10,22} We know of two calculations where, by contrast, ionization of the metal has been found: the reader is referred to Ref. 23, where Nb adsorbed on an O-terminated $\text{Al}_2\text{O}_{3+x}$ slab is seen to give $3e^-$ to the substrate, and Ref. 15, where the alkali metal K leaves $0.97e^-$ to the (001) surface of TiO_2 . In the first case, the substrate is non-stoichiometric, but carries an excess of half an oxygen layer. It is therefore natural for each excess oxygen atom to accept two electrons from the adsorbate. In the second case, the electron is transferred to the substrate, the corresponding state lying in the gap and being comparable to a state found on the reduced surface by the same authors.^{19,20} However, we believe this latter state to be an artefact of the pseudopotential method.¹¹ Here, our study yields electron transfers which are tenths of an electron, for coverages both with or without the additional degree of freedom given by LSDA. The actual geometries of metal adsorbate clusters on a rutile surface and the detailed atomic relaxations of the substrate atoms are obviously quite complex; moreover, they can be expected to vary depending on the adsorbed metal.²⁴ Still we found it could be interesting to see what occurs qualitatively on displacing the bridging oxygen and the titanium beneath it. The bridging oxygen was moved downwards by 0.12 a.u. and the titanium by 0.25 a.u. (following values given in Ref.

25). It was found that the total charge transfers are still at most two tenths of an electron, and that the same trend from reducing to oxidizing can be observed across the series. We therefore believe that the neglect of atomic relaxation is admissible.

The small charge transfers occurring in the systems under the present study differ radically from the examples quoted previously in this section,^{19,23} where the metal loses an integer number of electrons. In the case of K on the stoichiometric (001) surface of TiO_2 ,¹⁹ the geometry of the surface is different although the potassium atom is also adsorbed on top of a fivefold titanium. More importantly, K has a lower ionization energy than the metals in this study. It was found that a charge-transfer process occurs; ionization of the potassium is favored with the creation of gap states localized on the substrate. In our case, the system prefers to form metal-rutile bonds, and the energy position of these bonds, inside or just above the valence band, justifies *a posteriori* that such covalent bonds can be more favorable than higher titanium oxidation states. It might be useful to underline, though, that compared to delocalization of a whole $\text{K } e^-$ to the substrate, the individual charge transfer to the fivefold titanium is not so strikingly different: $0.34e^-$ in Ref. 19, 0.2 to $0.4e^-$ in our study. Although the absolute values of the charge transfers are small, they correlate with the trend of the adsorption energies, which do not follow the parabolic trend of the bond order. This emphasizes the importance of the electrostatic contribution in such systems.

In this model case, the appearance of a ‘‘new titanium state’’ can therefore correspond to quite different situations. With respect to surface spectroscopies, it was shown in Sec. III that, for example on the fivefold titanium, core-level shifts are predicted to occur especially for the ‘‘reactive’’ metals. We would like to point out that this is not associated with complete transfer of a metal d electron to the substrate, and that minimal variations of the charge transfer to the titanium can correspond to shifts of about 0.5 eV. We believe this can offer alternative interpretations to experiments such as Ref. 5; core-level shifts are seen in the early stages of Au deposition that disappear for a coverage larger than 1 ML. These were attributed to band-bending due to nucleation at defect sites. Our calculations show that shifts can occur without defects, and indeed without electron flow from the metal to the substrate. Therefore, it may be also that, at higher coverages, electrostatic shifts vanish as a consequence of changes in the Madelung potentials.

CONCLUSIONS

To summarize, our first-principles calculations of 5d transition-metal rows adsorbed on top of the fivefold titanium on the stoichiometric (110) surface of rutile give a detailed account of the changes induced by the metal on the substrate. Across the series, the relative alignments of the local densities of states vary, with the occurrence of band bending at the beginning of the series. The nobler metals are, as expected, more oxidizing. The varying part of the charge transfer is localized mostly on the bridging oxygen and on the fivefold titanium. We do not find that the variation from reducing to oxidizing across the series (Figs. 7 and 10) is associated with large changes in the substrate metal oxida-

TABLE III. Broken-row configuration: spin-polarized moments.

Metal	Metal moment	Ti(2) moment
Ta	2.737	0.271
W	3.825	0.173
Re	4.257	-0.001
Os	3.288	-0.110
Ir	2.046	-0.079
Pt	0.167	0.003
Au	0.000	0.001

tion state. There is a degree of flexibility for the fivefold titanium oxidation number, on the order of tenths of electrons, but no integer electron charge transfer from the metal atoms is seen. The bonding between the metal and the titanium beneath it is covalent in nature. Yet the trend of the variations of the adsorption energies suggests these variations are dominated by electrostatic effects; if they were dominated by the metal-titanium covalent bond, the trend would be opposite to here, where metals at the end of the series are more bonding. The numerous experimental studies of metal adsorption on TiO₂ include the 5d metals Pt and Au, but there is systematic data across the series for the 3d transition metals only. In this case the wetting ability of the metal seems greater for metals at the beginning of the series, which suggests that the adsorption energies are greater for

these metals. Assuming that such a picture is also valid for the 5d series, our results would point out that the number of valence electrons of the metal alone cannot account for stronger binding of reducing species. This would emphasize the fact that the adsorption site is likely to be a determining factor in the energetics.

ACKNOWLEDGMENTS

The authors wish to thank M. W. Finnis for valuable discussions and M. Methfessel for practical help. We also enjoyed discussions with D. L. Carroll and D. Bonnell. This work was funded by the Leverhulme Trust under Grant No. F/203/T.

*Present address: Centre Europeen de Calcul Atomique et Moleculaire (CECAM), E.N.S. Lyon, 46, allée d'Italie, F-69364 Lyon Cedex 07, France. Electronic address: tnle@cecam.fr

¹V. E. Henrich and P. A. Cox, *The Surface Science of Metal Oxides* (Cambridge University Press, Cambridge, 1994).

²R. Persaud and T. E. Madey, in *The Chemical Physics of Solid Surfaces and Heterogeneous Catalysis*, edited by D. A. King and D. P. Woodruff (Elsevier, City, 1997), Vol. 8.

³U. Diebold, J. M. Pan, and T. E. Madey, *Surf. Sci.* **331-333**, 845 (1995).

⁴S. Fischer, J. A. Martin-Gago, E. Roman, K. D. Schierbaum, and J. L. de Segovia, *J. Electron Spectrosc. Relat. Phenom.* **83**, 217 (1997).

⁵L. Zhang, R. Persaud, and T. E. Madey, *Phys. Rev. B* **56**, 10 549 (1997).

⁶D. L. Carroll, M. Wagner, M. Ruhle, and D. A. Bonnell, *Phys. Rev. B* **55**, 9792 (1997).

⁷D. L. Carroll, M. Wagner, M. Ruhle, and D. A. Bonnell, *J. Mater. Res.* **12**, 975 (1997).

⁸Z. M. Liu and M. A. Vannice, *Catal. Lett.* **43**, 51 (1997).

⁹M. W. Finnis, *J. Phys. C* **8**, 5811 (1996).

¹⁰I. Yudanov, G. Pacchioni, K. Neyman, and N. Rosch, *J. Phys. Chem. B* **101**, 2786 (1997).

¹¹A. T. Paxton and L. Thiên-Nga, *Phys. Rev. B* **57**, 1579 (1997).

¹²C. Noguera, *Physics and Chemistry of Oxide Surfaces* (Cambridge University Press, Cambridge, 1996).

¹³K. Nath and A. B. Anderson, *Phys. Rev. B* **39**, 1013 (1994).

¹⁴P. Alemany, R. S. Boorse, J. M. Burlitch, and R. Hoffman, *J. Phys. Chem.* **97**, 8464 (1993).

¹⁵M. Methfessel, *Phys. Rev. B* **38**, 1537 (1988); M. Methfessel, C. O. Rodriguez, and O. K. Andersen, *ibid.* **40**, 2009 (1989).

¹⁶K. D. Schierbaum, S. Fischer, M. C. Torquemada, J. L. de Segovia, E. Roman, and J. A. Martin-Gago, *Surf. Sci.* **345**, 261 (1996).

¹⁷U. von Barth and L. Hedin, *J. Phys. C* **5**, 2064 (1972); V. L. Moruzzi, J. F. Janak, and A. R. Williams, *Calculated Electronic Properties of Metals* (Pergamon, New York, 1978).

¹⁸A. P. Sutton and R. W. Balluffi, *Interfaces in Crystalline Materials* (Clarendon, Oxford, 1995); V. Heine, *Phys. Rev.* **138**, A1689 (1965).

¹⁹P. J. Lindan, J. Muscat, S. Bates, N. M. Harrison, and M. Gillan, *Faraday Discuss.* **106**, 135 (1997).

²⁰P. J. Lindan, N. M. Harrison, M. J. Gillan, and J. A. White, *Phys. Rev. B* **55**, 15 919 (1997).

²¹W. Mackrodt, E. A. Simson, and N. M. Harrison, *Surf. Sci.* **384**, 192 (1997).

²²U. Schönberger, O. K. Andersen, and M. Methfessel, *Acta Metall. Mater.* **40**, S1 (1992).

²³C. Kruse, M. W. Finnis, J. S. Lin, M. C. Payne, V. Y. Milman, A. De Vita, and M. J. Gillan, *Philos. Mag. Lett.* **73**, 377 (1996).

²⁴R. Heise and R. Courths, *Surf. Sci.* **333**, 1460 (1995).

²⁵M. Ramamoorthy and D. Vanderbilt, *Phys. Rev. B* **49**, 16 721 (1994).